

國立交通大學

電子工程學系 電子研究所碩士班

碩士論文

量化 MIMO 系統通道容量之研究與分析

Research and Analysis in Channel Capacity of
Quantized MIMO System

研究生：黃俞榮

指導教授：桑梓賢 教授

中華民國九十八年四月

量化 MIMO 系統通道容量之研究與分析

Research and Analysis in Channel Capacity of Quantized
MIMO System

研 究 生：黃俞榮

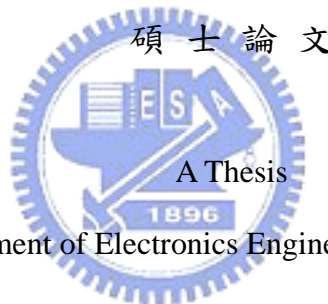
Student : Yu-Rong Huang

指 導 教 授：桑梓賢 教授

Advisor : Tzu-Hsien Sang

國 立 交 通 大 學

電子工程學系 電子研究所碩士班



Submitted to Department of Electronics Engineering & Institute of Electronics

College of Electrical and Computer Engineering

National Chiao Tung University

in Partial Fulfillment of the Requirements

for the Degree of

Master

in

Electronics Engineering

April 2009

Hsinchu, Taiwan, Republic of China

中 華 民 國 九 十 八 年 四 月

量化 MIMO 系統通道容量之研究與分析

研究生：黃俞榮

指導教授：桑梓賢 教授

國立交通大學

電子工程學系電子研究所碩士班

摘要



多重輸入多重輸出(MIMO)系統在過去數年,已被證實擁有許多好處,其中最主要的好處為增加頻寬效益(spatial multiplexing)和對抗通道衰減(spatial diversity),但過去對於 MIMO 系統的研究,甚少考慮接收端量化的問題,在實際的應用上,發射及接收的信號都是離散訊號。在這篇論文中,我們主要研究接收訊號經過量化後,MIMO 系統的通道容量,並且考慮簡單的 Relay Channels。

我們首先提出在傳送訊號有功率限制的情況下,且接收訊號經過量化的通道容量計算演算法,並且經由分析其最佳輸入信號的機率分布,說明且驗證演算法的正確性,接著用我們所提出的演算法模擬在不同的 MIMO 架構中所得到的通道容量且說明其結果,並且在傳送天線數以及調變信號固定的情況下,討論 AGC 使其可以得到最大的消息量。最後,我們分析簡單的 relay channel 經過量化後的通道容量。

Research and Analysis in Channel Capacity of Quantize MIMO System

Student : Yu-Rong Huang

Advisor : Tzu-Hsien Sang

**Department of Electronics Engineering & Institute of Electronics
National Chiao Tung University**

The logo of National Chiao Tung University is a circular emblem with a gear-like border. Inside the circle, there is a stylized figure holding a torch, and the year '1896' is inscribed at the bottom. The word 'ABSTRACT' is overlaid in large, bold, black capital letters across the center of the logo.

ABSTRACT

In the past few years, MIMO systems were already proven to have many advantages. The main advantages are spatial multiplexing and spatial diversity. In the past research, few have considered the problem of discrete signals at the transmitters and receivers; in this thesis, we study and analyze the capacity of quantized MIMO systems and consider the case of simple relays.

We propose an algorithm that can calculate Discrete-input and Quantized-output channel capacity with input power constraint and analyze the optimal input distribution. Then we run the algorithm to calculate channel capacity of different MIMO scenarios and explain the simulation results. Proper AGC scheme is also used to get the maximum information rate. Finally we consider simple relay channels and the simulated channel capacity is presented.

在這將近三年的研究所生涯中,學習了不少研究的方法與做人處事的道理。首先要感謝指導教授桑梓賢老師,除了專業上的指導與幫助,有時也會給予我一些思考方向上的激盪,使我更可以用不同的角度去思考問題。另外研究室的欣德學長也在有問題疑惑時,給予我很大的幫助,同學宇峰、建男,以及各位學弟的兩年同窗生活,除了解決研究上的問題外,也讓我的研生活多采多姿。最後要感謝我的父母親對我的支持與栽培,讓我的學生生涯畫下個句點。



Contents

Chapter 1 Introduction	1
1.1 Motivation	1
1.2 Literature Review	2
1.3 Purpose Of Research	8
Chapter 2 An Algorithm for computing the capacity of Discrete Input and Discrete Output MIMO channel with input power constraint	9
2.1 Quantized MIMO System	9
2.2 Algorithm	11
2.2.1 Algorithm Research	11
2.2.2 Interval halving procedure	13
2.2.3 Newton-Raphson procedure	14
2.2.4 Algorithm Convergence	14
Chapter 3 Simulation Result	15
3.1 Discrete-input and discrete-output MIMO Rayleigh flat-Fading channels	15
3.2 The maximum information rate about the discrete-input and discrete-output MIMO channel	17
3.3 Optimal input vector distribution for different input power constraint	20

3.3.1	Low power constraint	20
3.3.2	High power constraint	26
3.4	AGC to achieve the channel capacity	28
Chapter 4	Simple Relay Case.....	30
4.1	Introduction	30
4.2	Basic Memoryless Forwarding Strategies.....	31
4.2.1	Demodulate And Forward.....	31
4.2.2	Amplify And Forward	31
4.3	Simulation Results.....	32
Bibliography		36
About the Author		37



List of Figures

Fig. 1.1	Digital input and continued output AWGN channel model [4].....	2
Fig. 1.2	An uniform quantizer.....	3
Fig. 1.3	Simulation of 4X4 MIMO,4-QAM modulation. Result for different resolution of quantization is shown [7].....	5
Fig. 1.4	Quantized MIMO system model [7].....	5
Fig. 2.1	Quantized MIMO system model [7].....	10
Fig. 3.1	Simulation Results.....	16
Fig. 3.2	All possible transmit signal vectors in 2X2 quantized MIMO system.....	18
Fig. 3.3	Quantized signal vectors at the receiver.....	18
Fig. 3.4	Simulation result of a specific channel.....	19
Fig. 3.5	Simulation result for low input power constraint.....	23
Fig. 3.6	Low power constrain (power from low to high).....	24
Fig. 3.7	Optimal input distribution for high power constraint.....	26
Fig. 3.8	High power constrain (power from low to high).....	27
Fig. 3.9	Different AGC.....	29
Fig. 4.1	Elementary Relay Channel.....	30
Fig. 4.2	Different Parallel Relay.....	33
Fig. 4.3	Different Parallel Relay And No relay.....	33

Fig. 4.4 Different Relay Strategies.....34

Fig. 4.5 Different Received Antenna.....34

Fig. 4.6 Different Combination.....35

Fig. 4.7 Similar Performance With Different Combination.....35



List of Tables

Table 1.1	Literature summary.....	7
Table 3.1	Output vector and its possible input vectors.....	25



Chapter 1

Introduction

1.1 Motivation

Channel capacity, a fundamental concept in information theory, was introduced by Shannon [1] to specify the asymptotic limit on the maximum rate C at which information can be reliably conveyed by the channel. Any coding scheme that superficially appears to operate at a rate higher than C will cause enough data to be lost because of uncorrectable channel errors so that the actual information rate is not to be greater than C .

In [1], when computing the channel capacity the assumption is made that the channel inputs and the channel outputs can be treated as continuous random variables. Since the DSP hardware used in digital modems utilizes a finite signal set (channel input are modulation signals, such as QAM signals), and channel output are quantized signals, it is clear that the channel inputs and the channel outputs are not Gaussian random variables and the Shannon bound is not exact. So our research motivation is to propose an algorithm to modify the Shannon bound in the practical digital channels, and extend to MIMO channel.

1.2 Literature Review

The problem of obtaining the capacity of a discrete-input (fixed input constellations) and quantized-output (the output signal is quantized by quantizer) MIMO Rayleigh flat-fading channel has been preceded by such work as [1], in which Shannon calculated the capacity of an AWGN channel and showed that this capacity is achievable by a Gaussian input distribution. Arimoto [2] and Blahut [3] derived a numerical method for computing the capacity of discrete memoryless channels, but their algorithm did not support input power constraint. In [4], the Blahut-Arimoto algorithm is modified to incorporate an average power constraint, and is used to compute the capacity of discrete-input and continuous-output (output signals are not quantized) channel, and also the convergence is proved. The channel model in [4] is shown in Fig. 1.1.

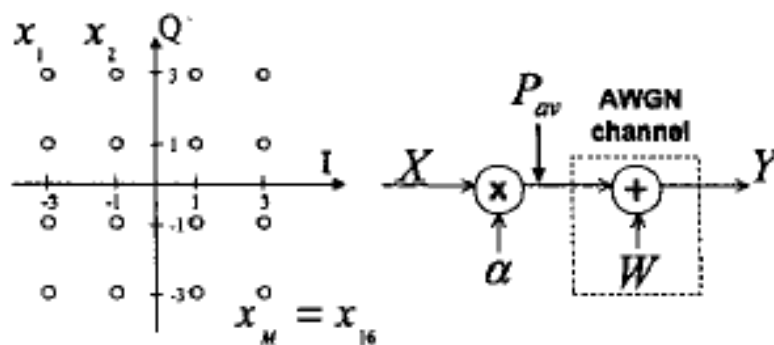


Fig. 1.1 Digital input and continued output AWGN channel model [4].

In [5], Bellorado extended the modified Blahut-Arimoto algorithm [4] (which

calculates the capacity of a discrete-input and continuous-output channel) to calculate the capacity of a MIMO Rayleigh flat-fading channel, which is also discrete-input and continuous-output channel. The algorithm becomes very computationally complex when the number of transmit antennas and signal set size grow; so the author makes a postulation that the MIMO channel is independent across antennas and dimensions (real dimension and imaginary dimension). Base on the postulation, the author proposed a new algorithm which drastically reduces the computation cost (for example, for 64-QAM constellations and three transmit antennas, a total of 262143 variables are evaluated in the old algorithm, while only 7 variables in the new algorithm).

In [6], Obianuju Ndili and Tokunbo Ogunfunmi discovered that the Shannon limit does not exist in modern communication systems (because of the DSP hardware used in digital modems utilizes a finite signal set), so they proposed the constrained Blahut-Arimoto algorithm to calculate the channel capacity with discrete-inputs (the input signals has not been modulated) and quantized outputs (the output signals was quantized by quantizer, which was shown in Fig. 1.2), and extended their algorithm to calculate the capacity of MIMO channels, but they did not prove the convergence of their algorithm.

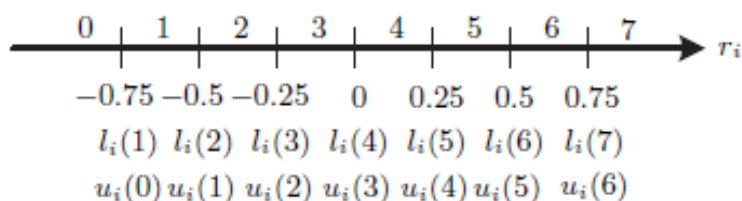


Fig. 1.2 An uniform quantizer

In [7], the author pointed out a question, a 64-QAM modulated signal received over a time-dispersive SISO (one transmit antenna and one receive antenna) channel with four multi-path components can very well be quantized by a 8 bit ADC ($4*64=256, \log_2 256=8$), which is sufficiently large for the modem to operate close to channel capacity. However, the reliance on fine ADC granularity easily becomes unjustified as soon as MIMO systems come into play. Consider for instance two data streams (two transmit antenna) of 64-QAM modulated signals received over a time-dispersive MIMO channel with four multi-path components. Now we need at least 14 bit ($\log_2(4*64*64)=14$) of resolution in order to obtain a fine granular quantization at each receive antenna. With increasing number of transmit antennas, the ADC resolution needed for fine granular quantization soon becomes infeasible in practice. But in their simulation (which is shown in Fig. 1.3), they showed that even coarse quantization leads to channel capacities which are surprisingly close to the ones obtainable with fine-granularity quantization. Their system model is shown in Fig. 1.4, where the transmit antennas transmit digital signal (such as QAM and PAM), and receive antennas quantized the received signals individually. Their method calculated the channel capacity by calculating the mutual information between \mathbf{X} and \mathbf{Y} (\mathbf{X} and \mathbf{Y} are vector), and letting the input distribution be uniform, shown in (1.1), so in their simulation, they did not get the optimal input distribution.

$$C = - \frac{1}{|M|} \sum_{j=1}^{|M|} \sum_{i=1}^{|Q|} pr[yi|xj] * \ln \frac{\frac{1}{|M|} \sum_{k=1}^{|M|} pr[yi|xk]}{pr[yi|xj]} \quad (1.1)$$

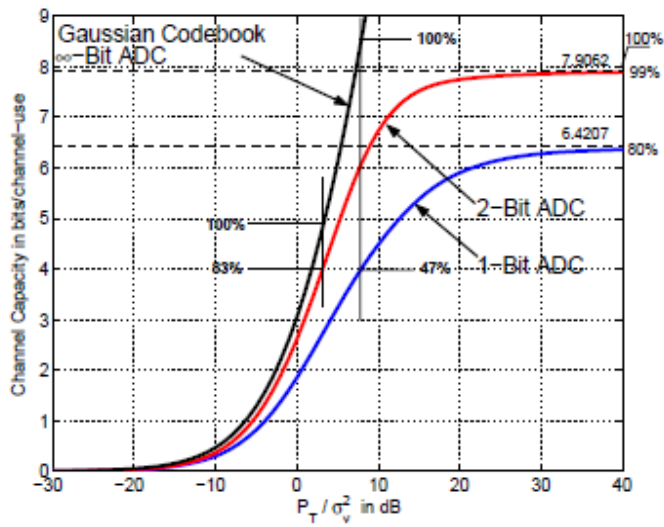


Fig. 1.3 Simulation of 4X4 MIMO,4-QAM modulation. Result for different resolution of quantization is shown [7].

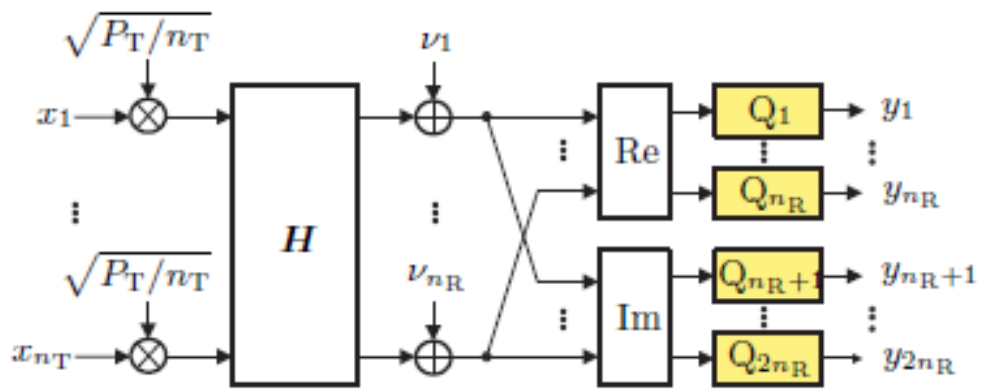


Fig. 1.4 Quantized MIMO system model [7].

According to these literatures, we classify the channel into four types.

- **Continuous-input and continuous-output**

The channel input is an analog random variable, and the channel output is also an analog random variable.

- **Continuous- input and discrete-output**

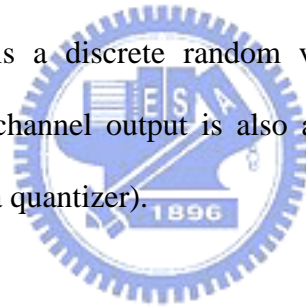
The channel input is an analog random variable, and the channel output is a discrete random variable (the output signal is quantized by a quantizer).

- **Discrete-input and continuous-output**

The channel input is a discrete random variable (the input signal is a modulation signal), and the channel output is an analog random variable.

- **Discrete-input and discrete-output**

The channel input is a discrete random variable (the input signal is a modulation signal), and the channel output is also a discrete random variable (the output signal is quantized by a quantizer).



In the end of this section, we summarize in Table 1.1 the different channel models.


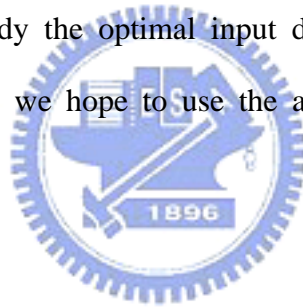
Channel model	Literature	Contribution
Continue input continue output	[1]	Assume channel input and channel output are Gaussian random variables, we can obtain the Shannon capacity bound for an AWGN channel
Continue input discrete output	No	No
Discrete input continue output	[4] [5] 	Propose an algorithm to calculate channel capacity with input power constraint, and extend the algorithm to calculate MIMO Reyleigh flat fading channel.
Discrete input discrete output	[2] [3] [6] [7]	Point out the question about quantized MIMO system with coarse quantization, and propose an algorithm to calculate the capacity.

Table 1.1 Literature summary

1.3 Purpose Of Research

In the previous section, we see that discrete-input and discrete-output channel model suits digital communication systems, but there is not an algorithm to calculate this channel capacity with input power constraint and a convergence proof (in [6], the authors proposed an algorithm, but they can not prove the convergence of the algorithm. In our simulations, we found case where their algorithm fails to converge.).

Our purpose of research is to propose an algorithm, which can calculate the discrete-input and discrete-output channel capacity with input power constraint, and guarantee the algorithm convergent, and the algorithm is extended to MIMO cases. We use the algorithm to study the optimal input distribution with different input power constraint. In the end, we hope to use the algorithm to study simple relay channel cases.



Chapter 2

An Algorithm for computing the capacity of Discrete Input and Discrete Output MIMO channel with input power constraint

2.1 Quantized MIMO System



Let us consider the quantized MIMO systems in Fig. 2.1, where n_T transmit antennas are connected to n_R receive antennas by the channel matrix $\mathbf{H} \in \mathbb{C}^{n_T \times n_R}$, which is assumed to be completely known to the transmitter and receiver. Because of knowing the channel state at the transmitter, we can get the optimal input distribution which is fitted the input power constraint ($\sum_i P_i \|\mathbf{X}_i\|^2 = P_{av}$) to approach the channel capacity. At every transmit antenna, the input signal $(x_1, x_2, \dots, x_{n_T})$ is the modulation signals (such as PAM and QAM), and the received signal is perturbed by samples $(v_1, v_2, \dots, v_{n_R})$ of complex, circularly symmetric, additive, white Gaussian noise of zero mean and variance of $\sigma_v^2/2$ in its real and imaginary part, respectively, yielding total noise power σ_v^2 . The receive signal is split up into real-part and imaginary-part and fed to the input of a bank of quantizers $Q_1, Q_2, \dots, Q_{2n_R}$ which

output the quantized signals $(y_1, y_2, \dots, y_{2n_R})$. Let us collect the input and output signals into vector

$$\mathbf{X}=[x_1, x_2, \dots, x_{n_T}]^T \in M \quad (2.1)$$

$$\mathbf{Y}=[y_1, y_2, \dots, y_{2n_R}]^T \in Q \quad (2.2)$$

Where M is a finite set containing all possible modulated transmit vector \mathbf{X} , while Q is a finite set containing all possible quantized receive vectors \mathbf{Y} . Let us write the input-output relationship of the quantized MIMO system as

$$\mathbf{Y}=\text{Quantized}(\mathbf{H}\mathbf{X}+\mathbf{V}) \quad (2.3)$$

The individual quantizer is defined by their input-output relationship as

$$\text{Quantized}(r_i)=q \quad \text{iff} \quad l_i(q) < r_i \leq u_i(q) \quad (2.4)$$

Where q is the output of the quantizers when its input ranges between a lower limit $l_i(q)$ and an upper limit $u_i(q)$, and these limits define the quantization interval for which the quantizers outputs the value q . Here we use the uniform quantizers in our simulation.

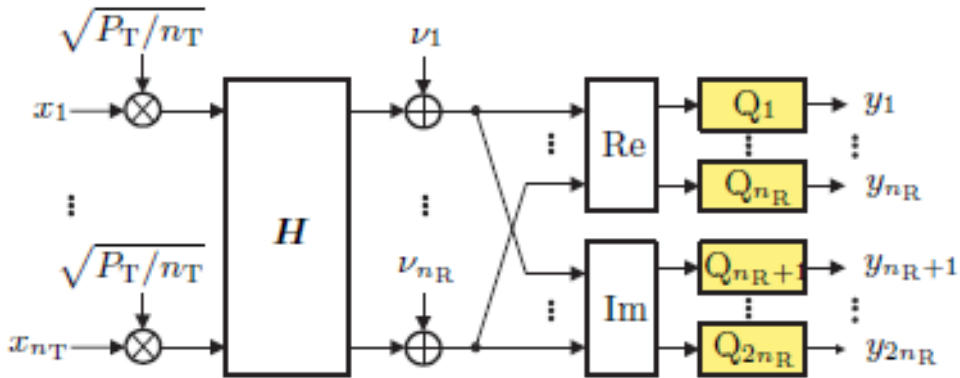


Fig. 2.1 Quantized MIMO system model [7].

2.2 Algorithm

2.2.1 Algorithm Research

Our goal is to find $P_X(\cdot)$ which maximize the information rate $\mathbf{I}(\mathbf{X};\mathbf{Y}|\mathbf{H})$. Here $\mathbf{I}(\mathbf{X};\mathbf{Y}|\mathbf{H})$ is the mutual information between channel input and channel output assuming the transmitter and receiver knows the channel matrix \mathbf{H} .

The discrete-input and discrete-output channel capacity computation problem is stated as follows:

Find the pmf (probability mass function) that satisfy the following equation

$$P_X^*(\cdot) = \arg \max_{P_X(\cdot)} \mathbf{I}(\mathbf{X};\mathbf{Y}|\mathbf{H}) \quad (2.6)$$

The maximization in (2.6) is taken under the following set of constraint.

$$\sum_{\mathbf{X}_i \in M} P_X(\mathbf{X}_i) * \mathbf{X}_i^H * \mathbf{X}_i \leq P_{av} \text{ input power constraint} \quad (2.7)$$

$$\sum_{\mathbf{X}_i \in M} P_X(\mathbf{X}_i) = 1 \quad (2.8)$$

Finally, we wish to evaluate C (the discrete-input and discrete-output channel capacity), defined as

$$C = \mathbf{I}(\mathbf{X}; \mathbf{Y} | \mathbf{H}) | P_X(\cdot) = P_X^*(\cdot) \quad (2.9)$$

An algorithm computing the discrete-input and continuous-output channel capacity has been proposed in [6]. We can regard the discrete-output as a special case of the continuous-output. With the idea, we propose a discrete-input and discrete-output version for computing the quantized MIMO channel capacity. We state as follows.

For a specific channel \mathbf{H}

Step1: Initialization

- $P_X(\cdot)$ is chosen as any valid pmf over $\mathbf{X}=[x_1, x_2, \dots, x_{nT}]^T$ (2.10)

Step2: Expectation

- For all $\mathbf{X}_i \in M$, compute

$$T_i = E_Y \left[\frac{P_{X|Y}(\mathbf{X}_i | \mathbf{Y})}{P_X(\mathbf{X}_i)} \log_2(P_{X|Y}(\mathbf{X}_i | \mathbf{Y})) \right] \quad (2.11)$$

Step3: Maximization

- For all $\mathbf{X}_i \in M$, compute

$$P_X(\mathbf{X}_i) = \frac{2^{T_i + \lambda \mathbf{X}_i^H \mathbf{X}_i}}{\sum_{k=1}^M 2^{T_k + \lambda \mathbf{X}_k^H \mathbf{X}_k}} \quad (2.12)$$

- Where λ is chosen to satisfy

$$\sum_{i=1}^{M^T} (\mathbf{P}_{av} - \mathbf{X}_i^H \mathbf{X}_i) * 2^{T_i + \lambda \mathbf{X}_i^H \mathbf{X}_i} = 0 \quad (2.13)$$

Repeat step2 and step3 until $P_X(\cdot)$ converges, and we can get $P_X^*(\cdot)$.

In step2, the value T_i can be determined from the probability $P_{Y|X}(\mathbf{Y} | \mathbf{X})$. When given \mathbf{H} and \mathbf{X} , $\mathbf{Y} \sim \mathbf{N}(\mathbf{H}\mathbf{X}, \sigma_v^2 \mathbf{I})$, thus knowing the quantization levels and appropriate decision regions, the complementary error function can be used to compute $P_{Y|X}(\mathbf{Y} | \mathbf{X})$.

In step3, λ is chosen to satisfy the specific equation, and we introduce two methods in next two sections.

2.2.2 Interval halving procedure

Interval halving procedure is an efficient method for solving equation $f(x) = 0$. The requirements for using this method is that there are two values x_1 and x_2 that satisfy $f(x_1)f(x_2) < 0$. Since $f(x_1)$ and $f(x_2)$ have opposite signs, we know by the intermediate value theorem that there exists a solution \tilde{x} and that $x_1 \leq \tilde{x} \leq x_2$, and with only $n+1$ function evaluations we can find a shorter interval of length $\varepsilon = |x_1 - x_2|2^{-n}$ that contains \tilde{x} , the procedure was described as follows.

Input: $x_1, x_2, f(x), \varepsilon$ (tolerance error)

Output: A solution to the equation $f(x) = 0$ that lies in an interval of length $< \varepsilon$

Repeat

Set $x_3 = (x_1 + x_2)/2$

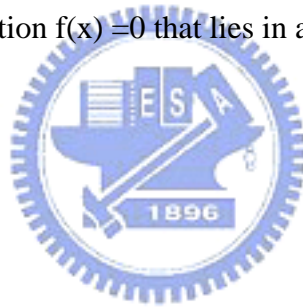
If $f(x_3)f(x_1) < 0$ Then

Set $x_2 = x_3$

Else Set $x_1 = x_3$

End If

Until $|x_1 - x_2| < 2\varepsilon$



2.2.3 Newton-Raphson procedure

Newton's method is perhaps the best known method for finding the roots of the real-value function. Newton's method can often converge quickly, especially if the iterations begin sufficiently near the desired roots.

Given a function $f(x)$ and its derivative $f'(x)$, we given a first guess x_0 , and a better approximation is

$$x_1 = x_0 - \frac{f(x_0)}{f'(x_0)} \quad (2.14)$$

We continue this process and can get the roots of the equation.

2.2.4 Algorithm Convergence



In this algorithm, we regard the discrete-output as the special case of the continuous-output, so we can see the convergence proof in [6].

Chapter 3

Simulation Result

3.1 Discrete-input and discrete-output MIMO

Rayleigh flat-Fading channels

In this section, we use the algorithm to simulate the discrete-input and discrete-output MIMO Rayleigh flat-fading channels. Two transmit antennas and two receive antennas (2X2 MIMO) are used, and at each transmit antenna, 4-QAM signal is transmitted, and at each receive antenna, a 3 bit quantizer is used. One thousand channels are randomly generated and the ergodic channel capacity is calculated through averaging. We show the simulation result in Fig. 3.1 (a).

Fig. 3.1 (a) shows a typical simulation. The capacity is saturates at high SNR because of the modulation scheme. Two antennas transmit independent signals, so the maximum capacity of this scheme is 4 bits/channel use ($2 * \log_2(4) = 4$). We show 2X1 and 2X2 MIMO performance in Fig. 3.1 (b).

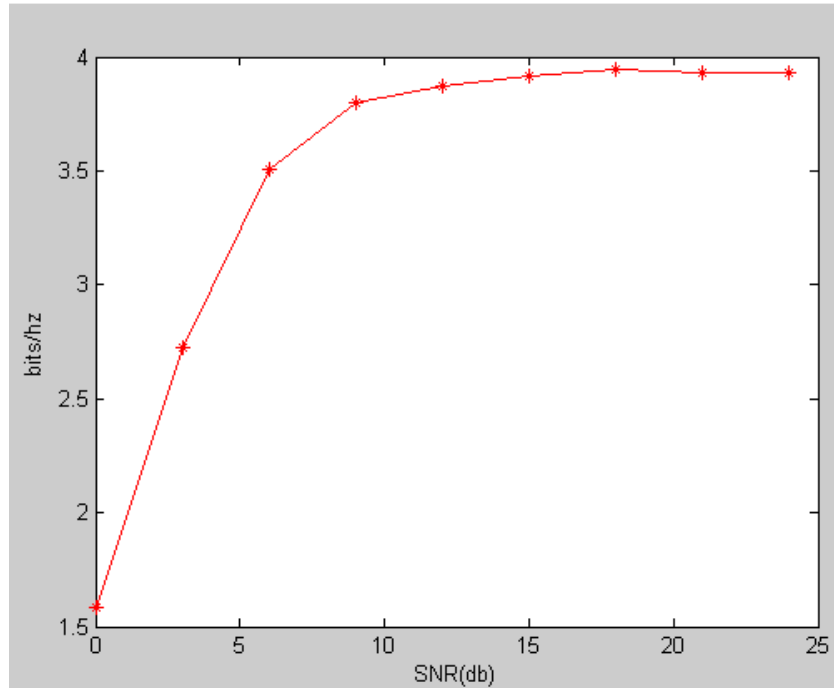


Fig. 3.1 (a) 2X2 MIMO, 4-QAM Modulation, 3 bit Quantizer

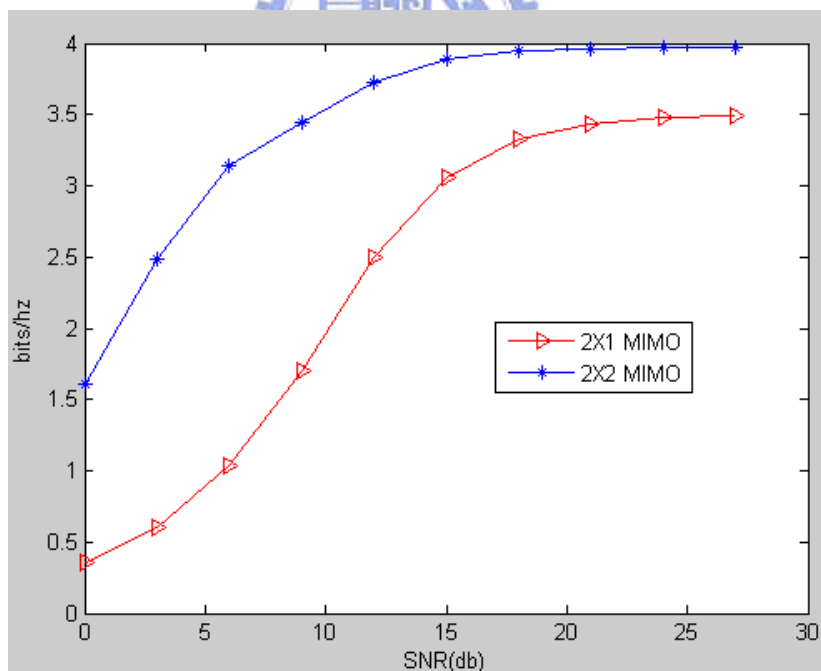


Fig. 3.1 (b) 2X1 and 2X2 MIMO, 4-QAM Modulation, 3 bit Quantizer

3.2 The maximum information rate about the discrete-input and discrete-output MIMO channel

Quantizing the signal at the receiver causes of the loss of information rate. If we transmit two independent 4-QAM signals at two antennas, and we can distinguish 16 ($4*4=16$) different signal vectors (which has two elements, and each element is 4-QAM signal), then the information rate is 4 bits/channel use. If we quantize the receive signals by quantizers, we may not distinguish the all difference at the receiver and get the maximum information rate. To explain this, we show all combination of two antenna and modulation signal (here we use a special 4-QAM signal, which real part is -1 and 5, and imagery part is -5 and 1) in Fig 3.2. We generate a channel randomly, then all the possible transmit signal vectors pass the channel and are quantized at the receiver, which was shown in Fig 3.3. In Fig 3.3, we can only distinguish 12 different signal vectors at the receiver, so the maximum information rate is 3.58 bit/channel use ($\log_2(12) = 3.58$). We run the algorithm, and show the simulation result in Fig 3.4, in which we see that the channel capacity does not exceed the maximum value 3.58.

```

tx_vec =

Columns 1 through 5

-1.0000 - 5.0000i -1.0000 - 5.0000i -1.0000 - 5.0000i -1.0000 - 5.0000i -1.0000 + 1.0000i
-1.0000 - 5.0000i -1.0000 + 1.0000i 5.0000 - 5.0000i 5.0000 + 1.0000i -1.0000 - 5.0000i

Columns 6 through 10

-1.0000 + 1.0000i -1.0000 + 1.0000i -1.0000 + 1.0000i 5.0000 - 5.0000i 5.0000 - 5.0000i
-1.0000 + 1.0000i 5.0000 - 5.0000i 5.0000 + 1.0000i -1.0000 - 5.0000i -1.0000 + 1.0000i

Columns 11 through 15

5.0000 - 5.0000i 5.0000 - 5.0000i 5.0000 + 1.0000i 5.0000 + 1.0000i 5.0000 + 1.0000i
5.0000 - 5.0000i 5.0000 + 1.0000i -1.0000 - 5.0000i -1.0000 + 1.0000i 5.0000 - 5.0000i

Column 16

5.0000 + 1.0000i
5.0000 + 1.0000i

```

Fig. 3.2 All possible transmit signal vectors in 2X2 quantized MIMO system.



```

Columns 1 through 5

-4.5000 - 4.5000i 4.5000 - 1.5000i -1.5000 - 4.5000i 4.5000 - 4.5000i -4.5000 - 4.5000i
4.5000 - 4.5000i 1.5000 - 1.5000i 4.5000 + 4.5000i 4.5000 + 4.5000i 4.5000 - 4.5000i

Columns 6 through 10

-1.5000 + 1.5000i -4.5000 - 4.5000i 4.5000 - 4.5000i -1.5000 - 1.5000i 4.5000 + 1.5000i
-1.5000 - 1.5000i 4.5000 + 4.5000i -1.5000 + 4.5000i 4.5000 + 1.5000i 4.5000 + 1.5000i

Columns 11 through 15

1.5000 5000i 4.5000 - 4.5000i -4.5000 5000i 1.5000 5000i -1.5000 - 4.5000i
4.5000 + 4.5000i 4.5000 + 4.5000i 4.5000 + 1.5000i -1.5000 + 4.5000i 4.5000 + 4.5000i

Column 16

4.5000 - 4.5000i
-1.5000 + 4.5000i

```

Fig. 3.3 Quantized signal vectors at the receiver.

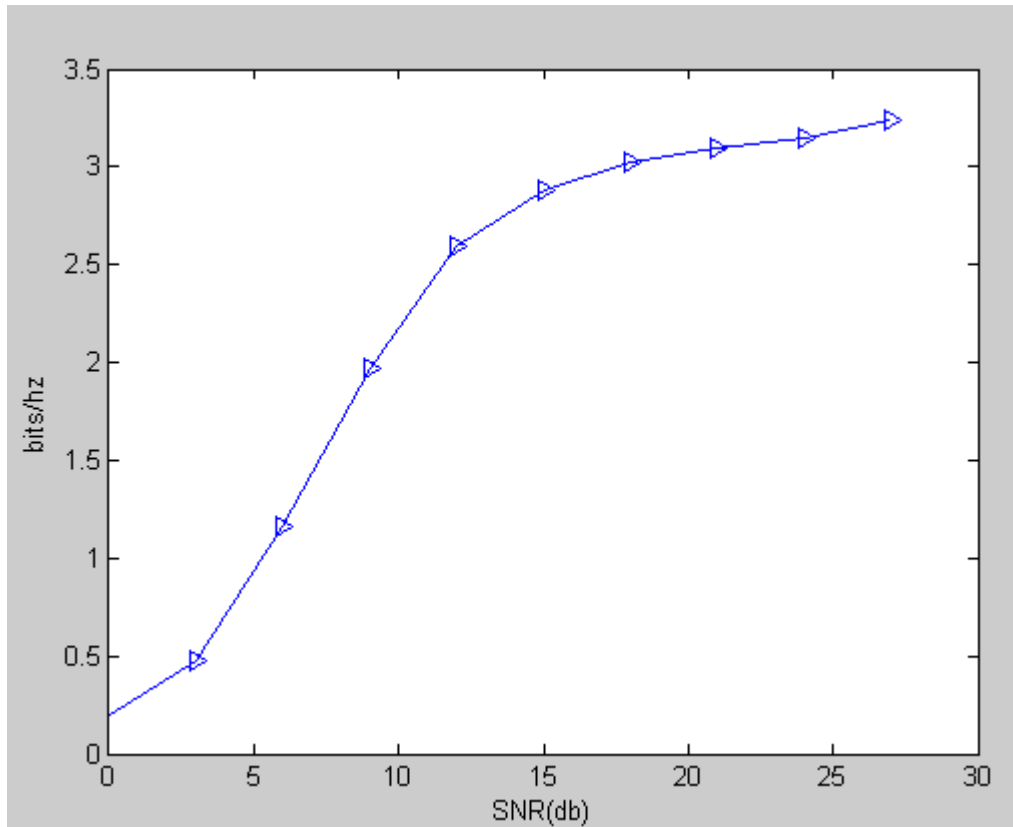


Fig. 3.4 Simulation result of a specific channel.



3.3 Optimal input vector distribution for different input power constraint

In this section, we analyze the optimal input vector distribution with different input power constraint in discrete-input and discrete-output MIMO Rayleigh flat fading channel. In our simulation, in order to observe the relationship between the power constraint and optimal input distribution, we use a special 4-QAM signal (which is the same in section 3.1). We analyze the optimal distribution with low power constraint in 3.3.1, and analysis high power constraint in 3.3.2.

3.3.1 Low power constraint

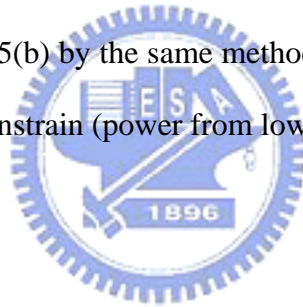


In this section, we analyze the optimal input vector distributions with low power constraint. We constrain the average input power 25 and show all possible transmit vector in Fig 3.5(a), and these transmit vectors pass a special channel is shown in Fig 3.5(b). In Fig 3.5(b), we see that we can only distinguish 4 different vectors (we circle in different color), so the maximum information rate is 2 bits/channel use ($\log_2(4) = 2$). We run the algorithm and show the simulation result in Fig 3.5(c). In 3.5(c), we see that the channel capacity is saturate at 2 bits/channel use. This result conforms to our anticipation. We show the optimal input vector distribution in high SNR in Fig 3.5(d). We analyze these distributions as follows.

In Fig 3.5(b), we see that we can only distinguish 4 different signal vectors, which are $(-1.5-4.5j, -1.5-4.5j)$, $(4.5-4.5j, 4.5-4.5j)$, $(-1.5+1.5j, -1.5+1.5j)$, and

$(4.5+1.5j, 4.5+1.5j)$.

When we receive the vector $(-1.5-4.5j, -1.5-4.5j)$, the transmit vector may be one of the three vectors (vector1 $(-1-5j, -1-5j)$, vector2 $(-1-5j, -1+j)$, vector5 $(-1+j, -1-5j)$). We summarize the relationship between the output vector and its possible input vectors in Table 3.1. From this table, we see that we receive the vector $(-1.5+1.5j, -1.5+1.5j)$ only when vector6 is transmitted, and vector6 has the lowest power $4(1^2 + 1^2 + 1^2 + 1^2 = 4)$, so that we see the probability of vector6 is the most in Fig 3.5(d). The three vectors (which are vector1, vector2 and vector5) are transmitted, then we can receive the vector $(-1.5-4.5j, -1.5-4.5j)$, but the vector2 and vector5 have the equal power 28, smaller than the power 52 of vector1, so that we see the probability of vector2 and vector5 are equal, and bigger than vector1. We can analysis the other distribution in Fig 3.5(b) by the same method. Fig 3.6 shows typical optimal distributions for low power constrain (power from low to high).



tx_vec =

Columns 1 through 5

-1.0000 - 5.0000i -1.0000 - 5.0000i -1.0000 - 5.0000i -1.0000 - 5.0000i -1.0000 + 1.0000i
 -1.0000 - 5.0000i -1.0000 + 1.0000i 5.0000 - 5.0000i 5.0000 + 1.0000i -1.0000 - 5.0000i

Columns 6 through 10

-1.0000 + 1.0000i -1.0000 + 1.0000i -1.0000 + 1.0000i 5.0000 - 5.0000i 5.0000 - 5.0000i
 -1.0000 + 1.0000i 5.0000 - 5.0000i 5.0000 + 1.0000i -1.0000 - 5.0000i -1.0000 + 1.0000i

Columns 11 through 15

5.0000 - 5.0000i 5.0000 - 5.0000i 5.0000 + 1.0000i 5.0000 + 1.0000i 5.0000 + 1.0000i
 5.0000 - 5.0000i 5.0000 + 1.0000i -1.0000 - 5.0000i -1.0000 + 1.0000i 5.0000 - 5.0000i

Column 16

5.0000 + 1.0000i
 5.0000 + 1.0000i



(a)

Columns 1 through 5

¹ ¹ ² ² ¹
 -1.5000 - 4.5000i -1.5000 - 4.5000i 4.5000 - 4.5000i 4.5000 - 4.5000i -1.5000 - 4.5000i
 -1.5000 - 4.5000i -1.5000 - 4.5000i 4.5000 - 4.5000i 4.5000 - 4.5000i -1.5000 - 4.5000i

Columns 6 through 10

³ ² ⁴ ² ²
 -1.5000 + 1.5000i 4.5000 - 4.5000i 4.5000 + 1.5000i 4.5000 - 4.5000i 4.5000 - 4.5000i
 -1.5000 + 1.5000i 4.5000 - 4.5000i 4.5000 + 1.5000i 4.5000 - 4.5000i 4.5000 - 4.5000i

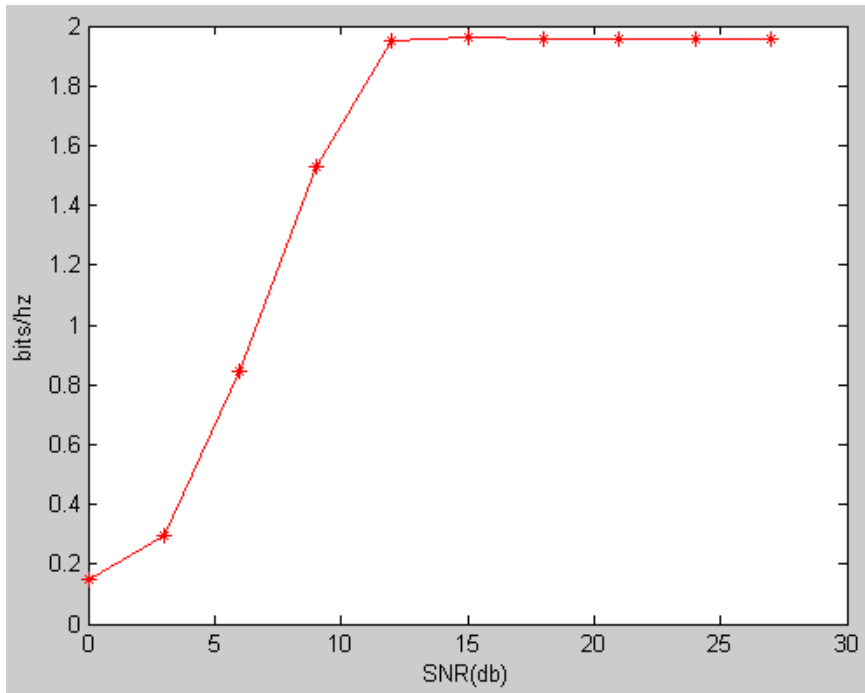
Columns 11 through 15

² ² ² ⁴ ²
 4.5000 - 4.5000i 4.5000 - 4.5000i 4.5000 - 4.5000i 4.5000 + 1.5000i 4.5000 - 4.5000i
 4.5000 - 4.5000i 4.5000 - 4.5000i 4.5000 - 4.5000i 4.5000 + 1.5000i 4.5000 - 4.5000i

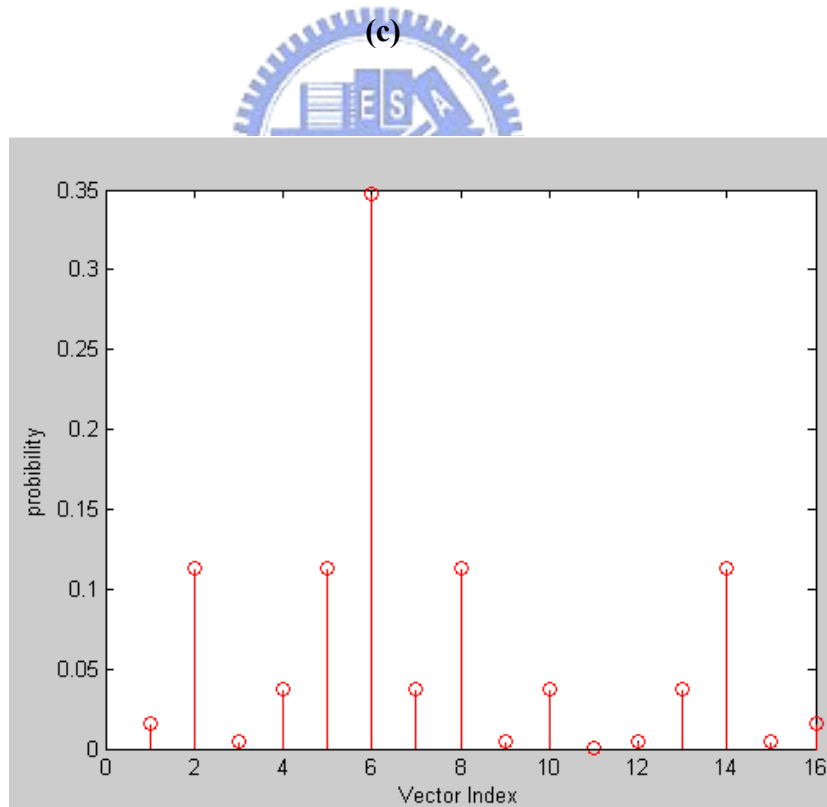
Column 16

⁴
 4.5000 + 1.5000i
 4.5000 + 1.5000i

(b)



(c)



(d)

Fig. 3.5 Simulation result for low input power constraint.

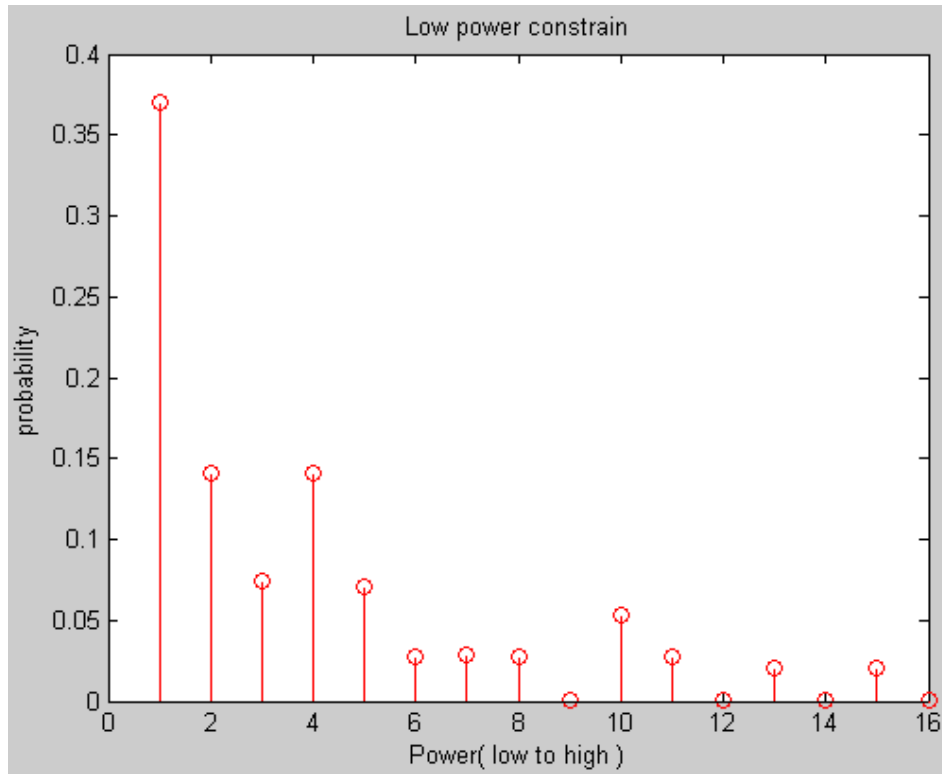


Fig. 3.6 Low power constrain (power from low to high)



Output vector	Possible input vectors
$(-1.5-4.5j, -1.5-4.5j)$	vector1 $(-1-5j, -1-5j)$, vector2 $(-1-5j, -1+j)$, vector5 $(-1+j, -1-5j)$
$(4.5-1.5j, 4.5-1.5j)$	vector3 $(-1-5j, 5-5j)$, vector4 $(-1-5j, 5+1j)$, vector7 $(-1+1j, 5-5j)$, vector9 $(5-5j, -1-5j)$, vector10 $(5-5j, -1+1j)$, vector11 $(5-5j, 5-5j)$, vector12 $(5-5j, 5+1j)$, vector13 $(5+1j, -1-5j)$, vector15 $(5+1j, 5-5j)$.
$(-1.5+1.5j, -1.5+1.5j)$	vector6 $(-1+1j, -1+1j)$
$(4.5+1.5j, 4.5+1.5j)$	Vector8 $(-1+1j, 5+1j)$, vector14 $(5+1j, -1+1j)$, Vector16 $(5+1j, 5+1j)$

Table 3.1 Output vector and its possible input vectors



3.3.2 High power constraint

In this section, we constrain the input average power 70 (high input power constraint), and the other settings are the same with section 3.3.1. We run the algorithm and show the optimal input vectors distributions in Fig 3.6. When we transmit one of the three vectors (which are vector8, vector14 and vector16), we can receive the vector $(4.5+1.5j, 4.5+1.5j)$. The vector16 has the most power of the three vectors, so we see that the probability of vector16 is the most. We can analysis the other distribution in Fig 3.7 by the same method. Fig. 3.8 shows typical optimal distributions for high power constrain (power from low to high).

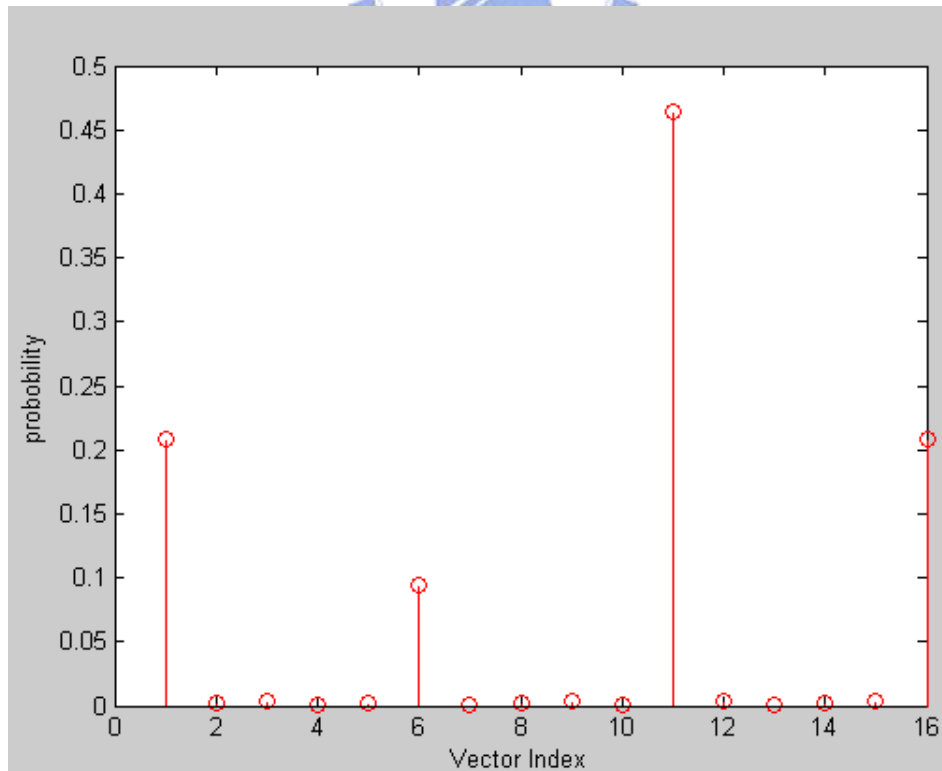


Fig. 3.7 Optimal input distribution for high power constrain.

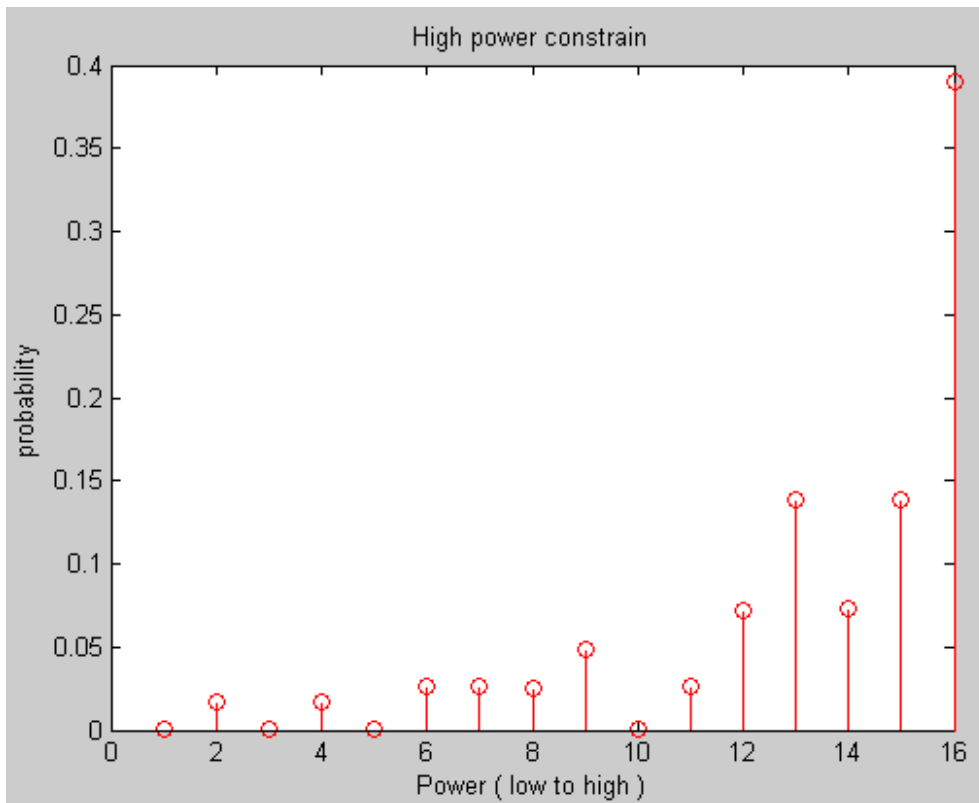
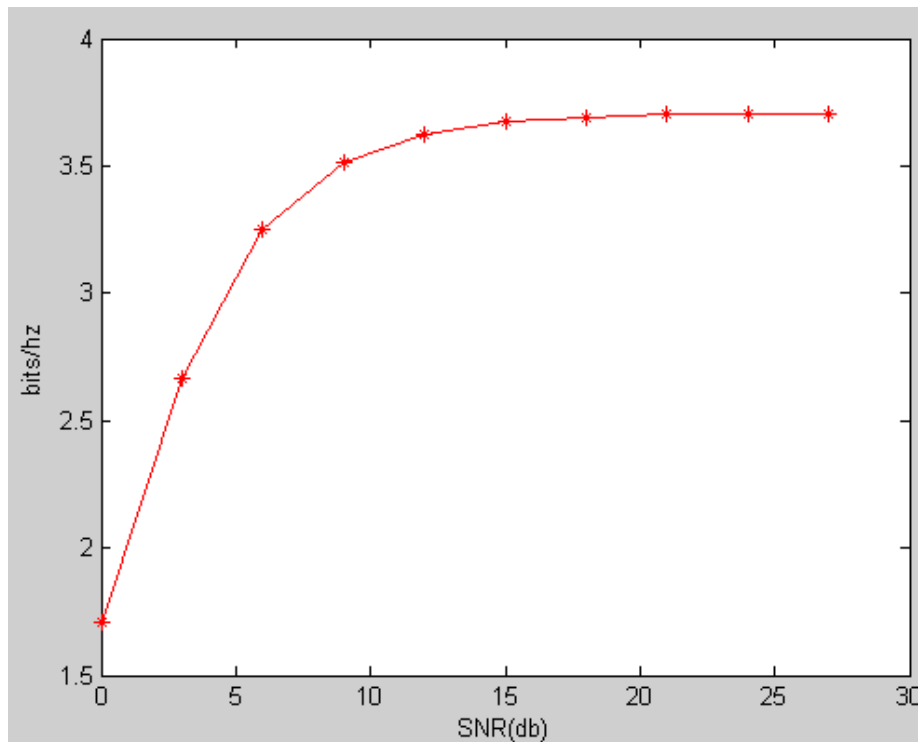


Fig. 3.8 High power constrain (power from low to high).

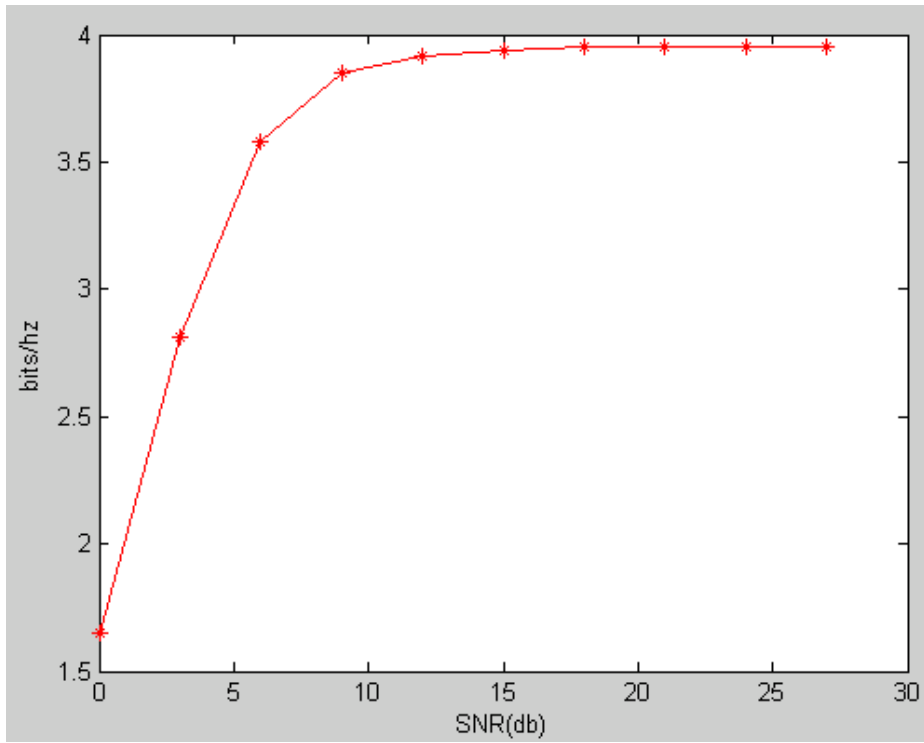


3.4 AGC to achieve the channel capacity

In our simulation, we discover that when we fix the antenna and modulation scheme, the AGC dominate the channel capacity. We show the different AGC in Fig. 3.9 and we can tune the AGC until achieve the maximum information rate.



(a) From -6 to 6



(b) From -3 to 3

Fig. 3.9 Different AGC



Chapter 4

Simple Relay Case

4.1 Introduction

Now, we want to use our algorithm to study cooperative communication and we only consider simple cases. We start with the elementary relay channel model as shown in Fig. 4.1, in which a single relay R assists the communication between the source S and the destination D. There is no direct link between the source and the destination.

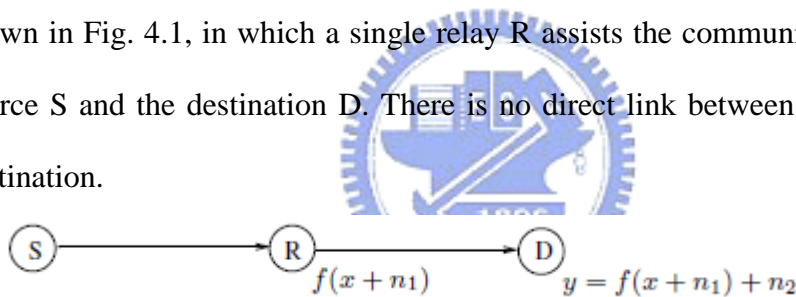


Fig. 4.1 Elementary Relay Channel

Let the transmit power at the source and the relay be p and p_R respectively. At both the relay and the destination, the receive symbol is corrupted by additive white Gaussian noise of unit power. Relay R observes r , a noisy version of transmitted symbol x . Based on the observation r , the relay transmits a symbol $f(r)$ which is received at the destination along with its noise n_2 . The relay function f satisfies the average power constrain ($E[|f(r)|^2] = P_R$).

$$r = x + n_1 \quad (4.1)$$

$$y = f(r) + n_2 \quad (4.2)$$

4.2 Basic Memoryless Forwarding Strategies

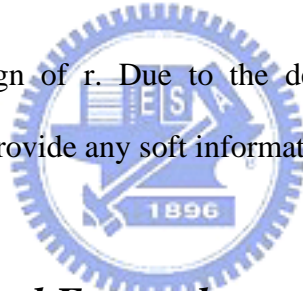
In this section, we introduce two basic memoryless forwarding strategies. We introduce demodulate forward in 4.2.1 and amplify forward in 4.2.2.

4.2.1 Demodulate And Forward

In DF protocol, demodulation of the received symbol at the relay is followed by modulation, the relay function for DF can be expressed as

$$f_{DF}(r) = \sqrt{P_R} \text{sign}(r) \quad (4.3)$$

where $\text{sign}(r)$ outputs the sign of r . Due to the demodulation process, the relay transmitted symbol does not provide any soft information to the destination.



4.2.2 Amplify And Forward

An AF relay simply forwards the received signal r after satisfying its power constraint.

The relay function for AF can be written as

$$f_{AF}(r) = \sqrt{\frac{P_R}{P+1}} r \quad (4.4)$$

Evidently, with AF, the relay tries to provide soft information to the destination. A disadvantage with this technique is that significant power is expended at the relay when $|r|$ is high.

4.3 Simulation Results

In this section, we consider simple relay case and Rayleigh flat-fading channel, and then run our algorithm. We set the total power (source and relay) S , and noise power N ($\text{SNR}=S/N$). Fig. 4.2 shows in Rayleigh flat-fading channel, more parallel relay get the better performance. Fig 4.3 shows one relay and no relay, the performance is similar, and two parallel relay is better. We compare two kind of different relay strategies we describe in section 4.2, and show the simulation results in Fig. 4.4, in which, we can see that DF get better performance in high SNR, because in high SNR relay demodulate received signals more correct. In Fig. 4.5, we show one relay and different received antenna simulation results, we can see that two received antennas get better performance. In relay systems, we can trade off number of relays, and quantization levels, and number of antennas. We show different relays and quantization levels in Fig. 4.6, in which we see that increase one antenna, get better performance than increase one-bit quantization. To achieve a specific performance, we can combination different relays, antennas and quantization levels. We show different combination achieve similar performance in Fig. 4.7.

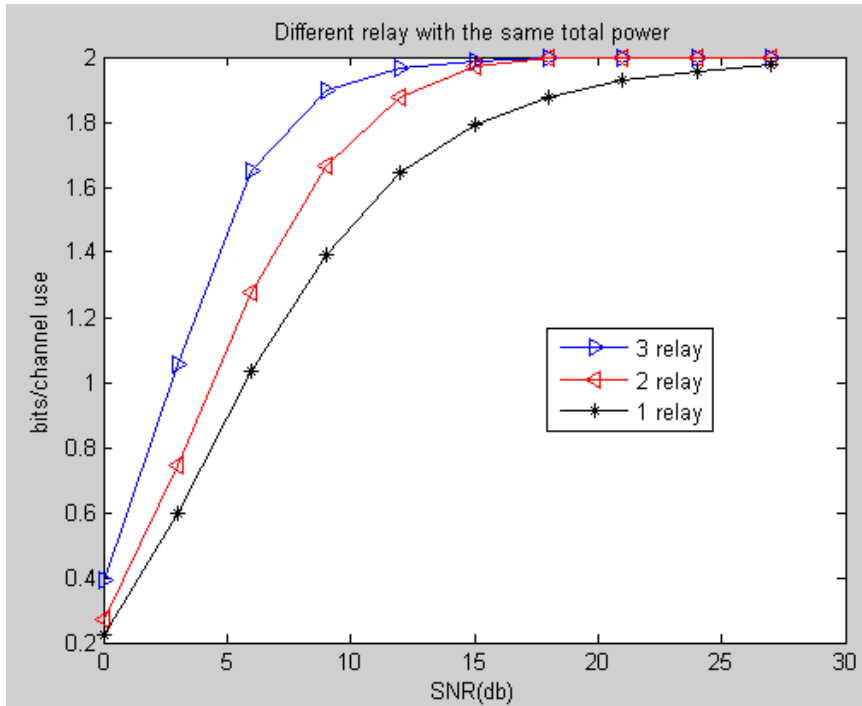


Fig. 4.2 Different Parallel Relay

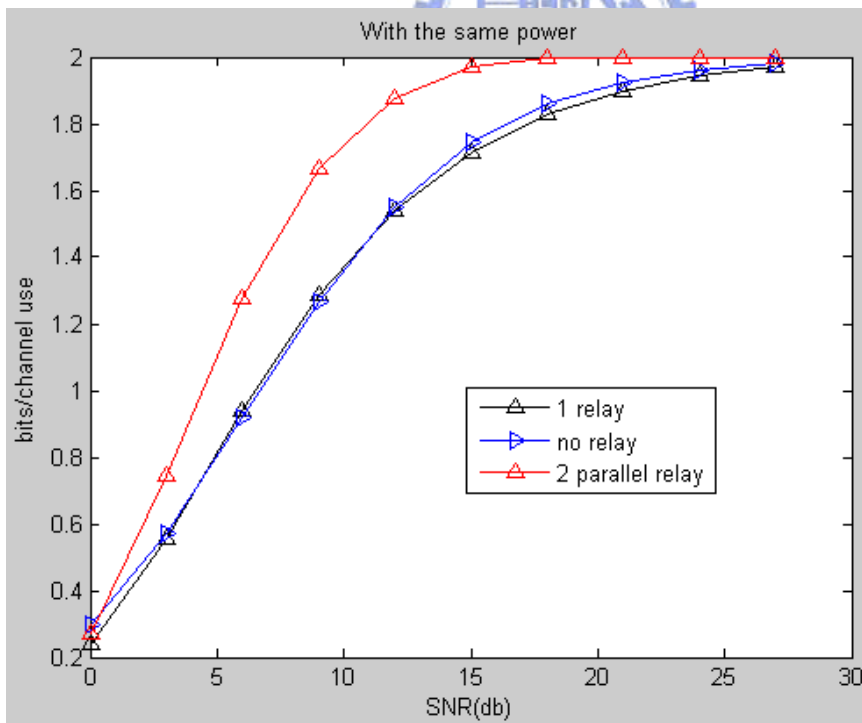


Fig. 4.3 Different Parallel Relay And No relay

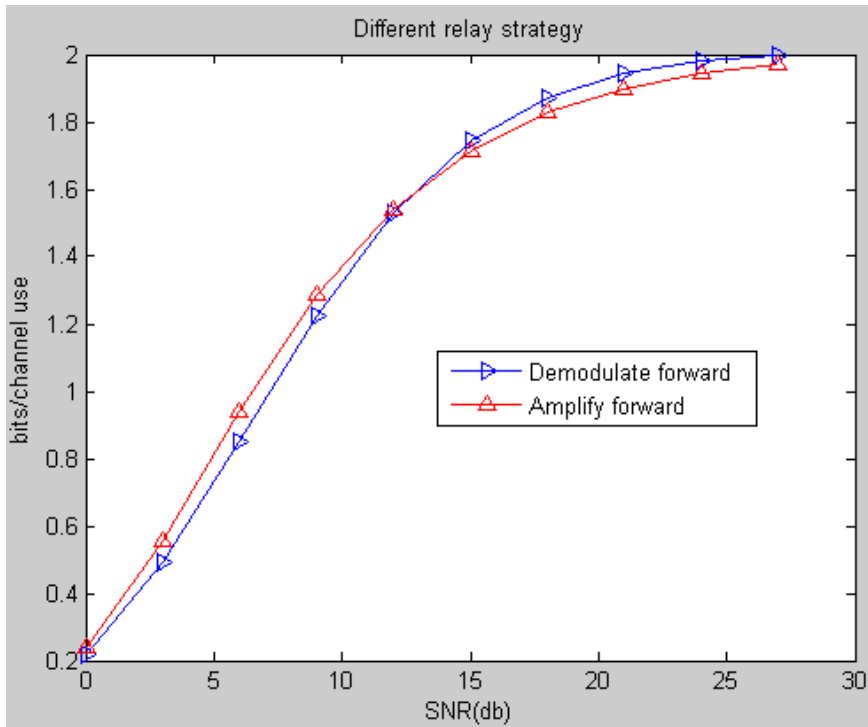


Fig. 4.4 Different Relay Strategies

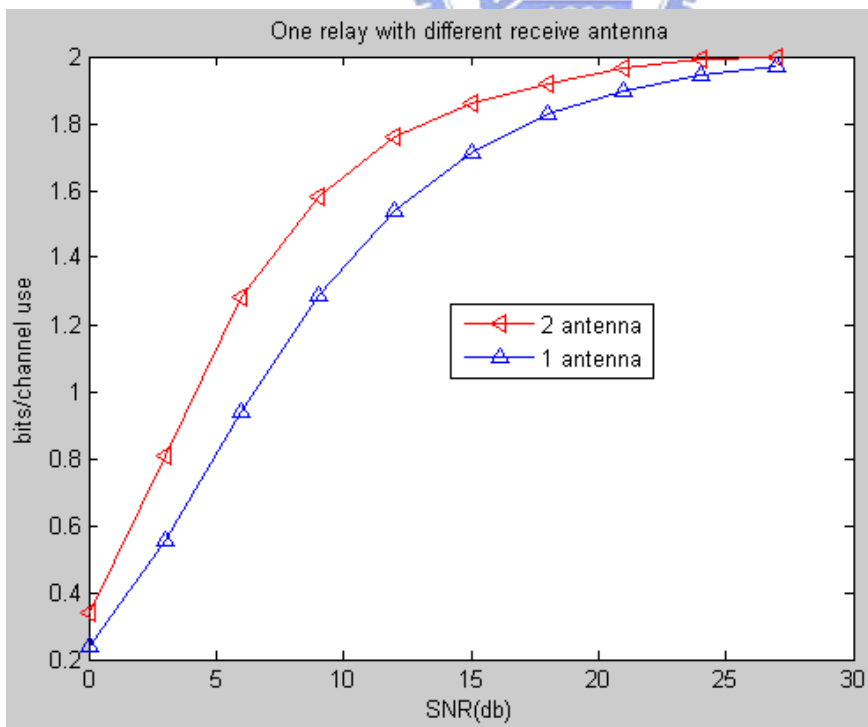


Fig. 4.5 Different Received Antenna

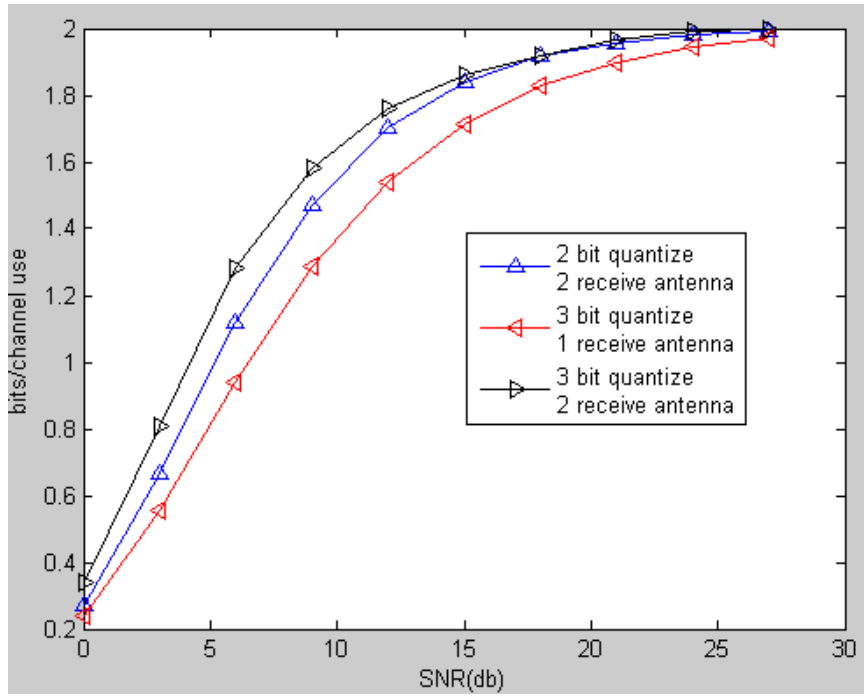


Fig. 4.6 Different Combination

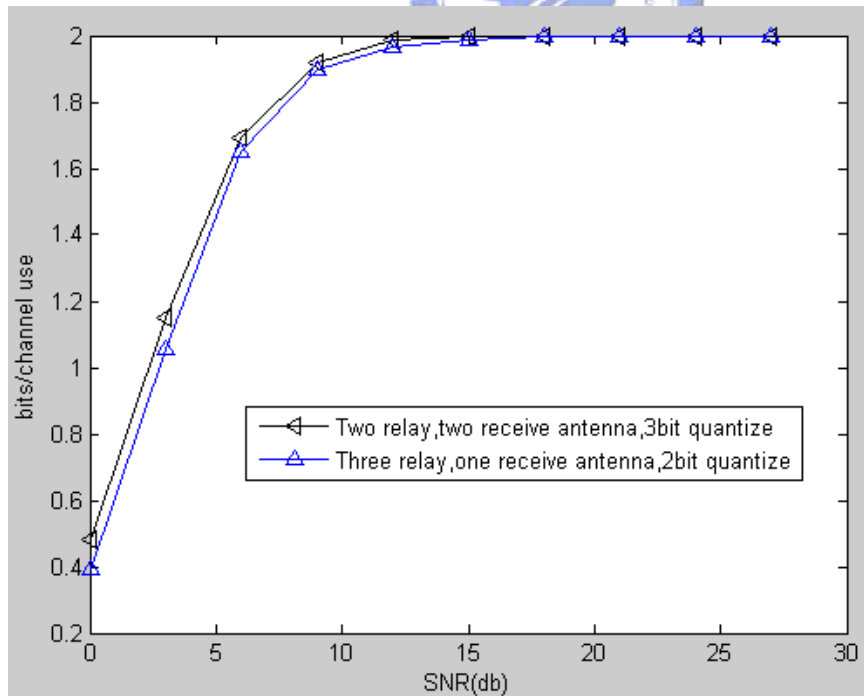


Fig. 4.7 Similar Performance With Different Combination

Bibliography

- [1] C. Shannon, "A mathematical theory of communication", Bell Syst. 1984.
- [2] S. Arimoto, "An algorithm for computing the capacity of arbitrary discrete memoryless channels", 1972.
- [3] R. E. Blahut , "Computation of channel capacity and rate distortion functions", 1972.
- [4] N. Varnica, X. Ma, and A. Kavcic, "Capacity of power constrained memoryless AWGN channels with fixed input constellations", November 2001.
- [5] J. Bellorado, S. Ghassemzadeh, and A. Kavcic, "Approaching the capacity of the MIMO Rayleigh flat-fading channel with QAM constellation, independent across antennas and dimensions".
- [6] Obianuju Ndili and Tokunbo Ogunfunmi, "Achieving Maximum possible Speed on Constrained Block Transmission System".
- [7] Josef A. Nossek and Michel T. Ivrlac, "Capacity and Coding for Quantized MIMO Systems", 2006.



About the Author

姓 名：黃俞榮 Yu-Rong Huang

出 生 地：高雄市

出生日期：1983. 11. 21

學 歷：

1990. 9 ~ 1996. 6 高雄市四維國小

1996. 9 ~ 1999. 6 高雄市私立復華中學

1999. 9 ~ 2002. 6 高雄市立中正高中

2002. 9 ~ 2006. 6 大同大學 電機工程學系 學士

